JOURNAL OF MATERIALS SCIENCE 30 (1995) 3358–3368

# The influence of residual stresses on the mechanical and thermal properties of injection moulded ABS copolymer

M. AKAY*, S. OZDEN
*Department of Mechanical and Industrial Engineering, University of Ulster at Jordanstown, Newtownabbey, Co. Antrim, BT37 0QB, UK*

The mechanical and thermal properties of acrylonitrile–butadiene–styrene copolymer (ABS) were determined for as-moulded and annealed specimens in order to assess the influence of residual stresses on these properties. Mouldings were heat treated at temperatures below and above the glass transition temperature, $T_g$. Annealing below the glass transition removes most of the residual stresses arising during the moulding process, while annealing above the glass transition temperature removes both the residual stresses and molecular orientation. Residual stresses have a strong bearing on the end-use properties. The thermal behaviour of the mouldings are mostly affected by the stimulation of molecular motion caused by the relaxation of the residual stresses near the glass transition temperature.

## 1. Introduction

The rate of cooling of the polymer mouldings affects its microstructure and hence its mechanical properties. Uneven cooling introduces residual stresses (RS) on the finished parts, which may cause failure during service life [1]. RS may lead to premature failure when superimposed on additional stresses caused by environmental effects.

The combination of residual stresses and molecular orientation and their variation through the thickness of the specimen impart variations on the properties of the mouldings. There have been extensive studies of the mechanical and thermal properties of injection moulded thermoplastics [2–20]. Residual stresses, particularly at the surface of the injection mouldings, are known to have improved impact strength [3], fatigue behaviour [4] and resistance to environmental stress cracking [2].

So and Broutman [3] examined the influence of residual stresses on the behaviour of quenched and annealed polycarbonate (PC) and polymethylmethacrylate (PMMA) plates. The Izod impact strength of quenched PC plates increased by a factor of ten compared to annealed ones. So and Broutman argue that the introduction of compressive stresses at the surface enhances the impact strength by increasing the transition thickness at which the failure mode changes from plane stress to plane strain. Quenched PMMA specimens were found to exhibit greater ductility than annealed ones under flexural loads.

Broutman and Krisknakumar [6] examined the effects of residual stresses on the Izod impact strength of PC, polyvinylchloride (PVC), ABS, PMMA and polysulfone. The increase in impact strength of PC was attributed to the craze suppression effect of the compressive residual stresses at the surface of the mouldings. Polysulfone and PVC sheets seemed to behave similarly to PC, while ABS and PMMA were not influenced by the quenching.

Siegmann *et al.* [2] investigated the effects of the residual stresses on crazing and softening behaviours of polystyrene (PS) and PMMA quenched from various temperatures into iced water. Both PS and PMMA showed decreased heat deflection temperatures as the magnitude of the residual stresses increased. It was concluded that the presence of residual stresses through the material thickness accelerated the softening of the polymers. The presence of the tensile residual stresses in the core was thought to increase the amount of the free volume.

Kamal and Lafleur [21] predicted the development of molecular orientation in high density polyethylene using the birefringence method. Molecular orientation was maximum beneath the surface, where maximum shear stresses were observed during the melt-fill. The level of orientation decreased gradually from beneath the surface towards the core. The shear stresses applied to the melt during injection moulding were assumed to be partly frozen as the melt solidified. The tensile modulus of elasticity was predicted using these frozen-in stresses and molecular orientation. Kamal and Lafleur predicted higher tensile modulus just below the surface, which sharply dropped, then stabilized towards the centre. Similar results were obtained subsequently by Fleischman [22].

Hoare and Hull [9] determined deformation and fracture behaviour of injection moulded polystyrene and the results were interpreted in terms of molecular orientation, crazing and shear yielding. The molecular orientation was characterized by birefringence, and

* To whom correspondence should be addressed.



0022–2461 

tensile tests were conducted on samples cut at different angles to the melt-fill direction. Maximum birefringence readings were obtained just beneath the surface of the samples, which was attributed to the presence of maximum orientation. The molecular orientation was observed to suppress craze nucleation in the melt-fill direction.

Dalal and Moet [10] investigated the tensile behaviour of 2,6 dimethyl poly(phenylene oxide) as a function of post-process annealing. Thin films (5–7 μm) were heat treated at 200 °C, which is below the $T_g$ (217 °C) of the material. Annealed specimens exhibited increased embrittlement and density increases.

Daane and Matsuoka [13] investigated the change of dynamic mechanical properties of ABS with temperature. Transitions were recorded at − 90 °C, as well as at 90 °C. Although the butadiene particles were dispersed through the glassy styrene–acrylonitrile matrix, both parts retained their thermomechanical properties. While the transition at 90 °C was the $T_g$ of ABS, the transition at − 90 °C was believed to be due to the rubbery butadiene particles. The samples with orientation exhibited a further transition at − 130 °C, which was thought to be due to the dilatation of rubber particles into the styrene–acrylonitrile matrix. The increase in the toughness of orientated ABS was attributed to the improved dispersion of rubber particles through the glassy matrix. It was argued that dispersion of the butadiene particles through the glassy matrix increased the yielding capacity of ABS, and the material failed in a ductile manner under tensile loads.

Rohn and Herh [23] compared the transition temperatures of as-injection moulded and post-injection heat treated ABS specimens. A main transition at 90 °C and a second transition at − 90 °C was obtained, as in the work of Daane and Matsuoka. The second transition was attributed to the rubbery part of ABS. On the other hand, the heat treated specimens exhibited an additional transition at − 130 °C. This result is in disagreement with Daane and Matsuaka [13] who obtained the same peak when the molecules were highly orientated, and attributed this to the dilatation of the rubbery particles through the glassy matrix in orientated condition. The as-moulded specimen exhibited higher loss factors at $T_g$. Although the authors argue that the orientation is removed by annealing at a temperature slightly above $T_g$, it is widely accepted that orientation can only be relaxed at temperatures significantly above $T_g$ because of the wide temperature span associated with the transition. It is more probable that the difference in the behaviour of ABS upon heat treatment is due to residual stresses rather than orientation.

The literature shows that the thermomechanical properties of polymers are largely influenced by the presence of residual stresses, as well as molecular orientation. The elastic modulus, heat deflection temperature and free volume content of the polymers are influenced by the presence of residual stresses. The skin–core structure (especially significant in semicrystalline polymers) of the injection mouldings causes material property gradients through the thickness of the samples. The relationship between the residual stresses and the thermal and mechanical properties are two-fold: while the residual stresses affect the thermomechanical properties, the development of the residual stresses may also be influenced by thermal and mechanical anisotropies through the thickness of the mouldings. It is thought that for a thorough understanding of the significance of the residual stresses in injection moulded specimens, assessment of reciprocal influences of residual stresses and the material properties become important.

## 2. Experimental procedure

### 2.1. Material and processing

A rectangular (pin) end-gated mould of $3 \times 76 \times 150\ mm^3$ dimensions and a mould for the production of dumbbell specimens were employed for the injection moulding of ABS (General Electrics' CYCLOC T 35) on a Stubbe SKM 51 injection moulding machine. The machine was set at 183 MPa injection pressure, 3 MPa back pressure, $250\ r\ min^{-1}$. screw rotational speed, 1 s injection time, 20 s cooling time, 3 s hold time, barrel temperature profile of 230, 240, 250 and 260 °C and 60 °C mould temperature.

A number of mouldings were annealed below $T_g$ (110 °C) at 80 °C for 24 h under vacuum and designated 'medium heat treated'. It was aimed to relieve as many thermal stresses as possible without affecting molecular orientation. Some of the medium heat treated mouldings were further heated at 135 °C for 12 h and designated 'full-heat treated'.

### 2.2. Test methods

#### *2.2.1. Mechanical tests*

Dumbbell specimens of gauge length 65 mm, thickness 3 mm and the width of the narrow portion of 10 mm were moulded and tensile tested according to ASTM D638-89 on an Instron 6040 machine. An extensometer was employed for the elastic modulus measurements at a test speed of $6.5\ mm\ min^{-1}$ to provide a strain rate of $0.1\ min^{-1}$. The remaining tensile tests were conducted at $10\ mm\ min^{-1}$.

Layers of 0.20 mm thickness were removed from the dumbbell shaped mouldings at different locations through the thickness and tensile tested as outlined above. Layer removal was conducted on a milling machine. The mouldings were held flat by vacuum and machined with a high speed single point cutter at $1500\ r\ min^{-1}$ and a feed rate of $120\ mm\ min^{-1}$. Some of the layers were used for density measurements to obtain a through thickness density profile.

The three-point flexural properties were determined according to ASTM D790M-86 at $12\ mm\ min^{-1}$ test speed and a span length of 54 mm using $3 \times 10 \times 80\ mm^3$ specimens. The flexural and tensile tests were conducted at approximately 22 °C and 63% relative humidity.

Notched impact properties were determined according to ASTM D256-88 using Charpy type test pieces. Specimens of $3 \times 10 \times 60\ mm^3$ were prepared from the moulded tensile bars and striked edge-on in three-point bending mode on a support span of

40 mm. Notches of 3 mm were milled with a 45° multiple point cutter of 0.25 mm radius. The tests were conducted on an instrumented impact testing machine. The system was based on a free fall of a weight from a specified distance. A 5 kg mass and a 45° triangular striking head with 3 mm tip radius was employed at an incident speed of 1.3 m $s^{-1}$.

The plaque mouldings were also drop weight impact tested with a hemispherical striker of 12.7 mm diameter. The specimens were freely supported on a rigid tube of 40 mm internal and 90 mm external diameter and impacted with a mass of 10 kg at a speed of approximately 3.8 m $s^{-1}$.

### 2.2.2. Thermomechanical tests

Dynamic mechanical thermal properties of as-moulded, medium heat treated and full heat treated mouldings were determined by means of a Du Pont Dynamic mechanical analyser (DMA) employed in fixed frequency mode. The specimens of $3 \times 10 \times 50\ mm^3$ dimensions were tested at a clamp separation of 30 mm, an oscillation amplitude of 0.7 mm, fixed frequency of 1 Hz and 3 °C $min^{-1}$ temperature increase rate. Dynamic mechanical tests were also conducted on 0.30 mm thick layers taken from the surface and core regions of the mouldings. In this case the oscillation amplitude was increased to 1.6 mm and the clamp separation was reduced to 4.5 mm for satisfactory tests. This arrangement was necessitated in order to increase the response of the equipment, which dramatically dropped because of reduced stiffness of thin samples.

The heat distortion temperature (HDT) of the mouldings was obtained in accordance with ASTM D648, which describes HDT as the temperature at which the specimen ($3 \times 13 \times 127\ mm^3$) deflects by 0.25 mm under 1820 kPa stress, while heated in an oil bath at a rate of 1.8–2 °C $min^{-1}$.

The linear thermal expansion of ABS samples were determined according to ASTM E288-88 by means of a Perkin–Elmer silica length dilatometer. The dilatometer is based on the principle of measuring the changes in length of the sample relative to a quartz tube using an linear voltage differential transducer (LVDT). The length dilatometer consists of a specimen chamber and a head fitted with an LVDT. The specimen is placed inside the quartz tube and both are moved to the bottom of the chamber. A quartz rod is placed to the top of the specimen. Upon heating, the plastic expands and pushes the quartz rod, which is at one end connected to the LVDT, while its other end rests on the specimen. The displacement of the quartz rod is registered by the LVDT.

### 2.2.3. Density measurements

The density measurements were obtained in accordance with ASTM D1505-85. A linear density column ranging from 1 to 1.2 g $cc^{-1}$ was prepared using sodium bromide–water solutions. The columns were set to stabilize at 23°, then the samples were put into the column and the readings were taken after 24 h. The method enables measurements to an accuracy of $1 \times 10^{-4}$ g $cc^{-1}$. Density measurements were conducted on specimens representing complete plaques and also on 0.20 mm thick specimens removed at different depths from the surface to the core of the plaque mouldings.

## 3. Results and discussion

### 3.1. Tensile and flexural properties

Residual stress distributions through the thickness of the ABS mouldings are presented elsewhere in detail [24]. Fig. 1 shows a typical through the thickness residual stress profile. As-moulded specimens were annealed to different extents in order to remove frozen-in residual stresses and any molecular orientation, so that an examination of the influence of these parameters on properties may be made.

Modulus of elasticity and tensile yield strength data for various ABS specimens are presented in Fig. 2. The values represent an average of at least five measurements. The modulus of elasticity increases with annealing time because of a possible increase in molecular packing resulting from the relief of residual tensile stresses. This is corroborated by density measurements

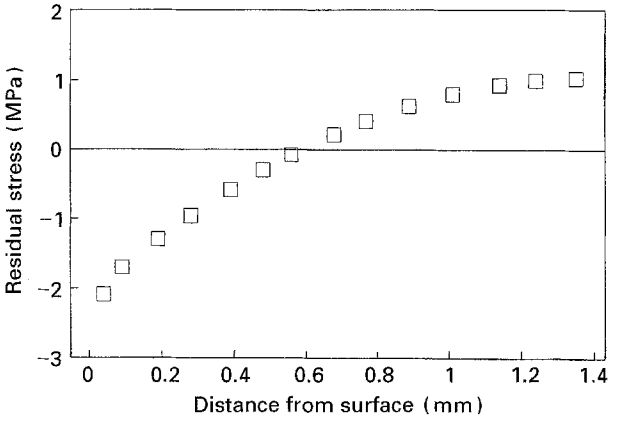


*Figure 1* Through the thickness residual stresses distribution of injection moulded ABS.

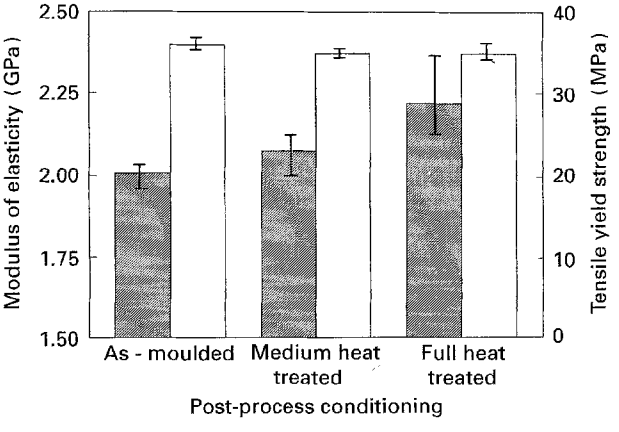


*Figure 2* Tensile properties versus post-process conditioning: (▩) modulus of elasticity, and (□) tensile yield strength.

(see Fig. 3). The density increased slightly upon heat treatment. The through the thickness density measurements, Fig. 4, show that the skin has a higher density than the core. This trend fits the notion that the compressive stresses at the surface force the molecules to pack more closely together; the interior tensile stresses tend to decrease the packing of the molecules by pulling them apart [2]. There is negligible variation in tensile yield strength with annealing. The force–displacement curves shown in Fig. 5 and the elongation at break values (see Fig. 6) indicate that as-moulded ABS specimens exhibit much greater ductility than the medium and full heat treated specimens.

The tensile fracture surface for as-moulded ABS is shown, Fig. 7. Medium and full heat treated specimens also revealed similar fracture surface patterns. The cracks start from the surface and progress toward the centre of the specimen. The magnified picture of the crack initiation and propagation regions (see Fig. 8) shows teardrop features, which indicates ductile failure rather than brittle failure [25]. There are no obvious striations associated with the crack propagation, usually observed in brittle failures. The compressive stresses at the surface are believed to delay the propagation of the cracks, which originate at the surface and, thus, allow the material around the crack to yield before the crack reaches its critical length, causing premature failure. The black spots in Fig. 8b are believed to be caused by dust particles.

Tensile modulus of elasticity as a function of distance from surface is presented in Fig. 9. The surface region reveals a higher modulus value than the core. A reduction of about 22% in modulus of elasticity was observed away from the surface. The high modulus value at the surface is due to higher molecular orientation near the surface and the presence of compressive residual stresses which reach a maximum right at the

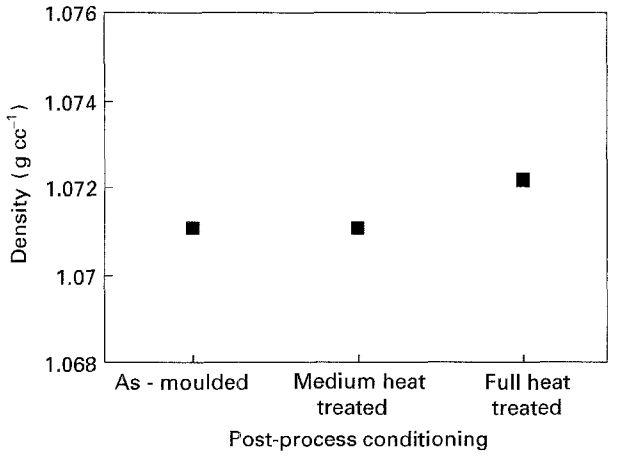


*Figure 3* Density of ABS versus post-process conditioning.

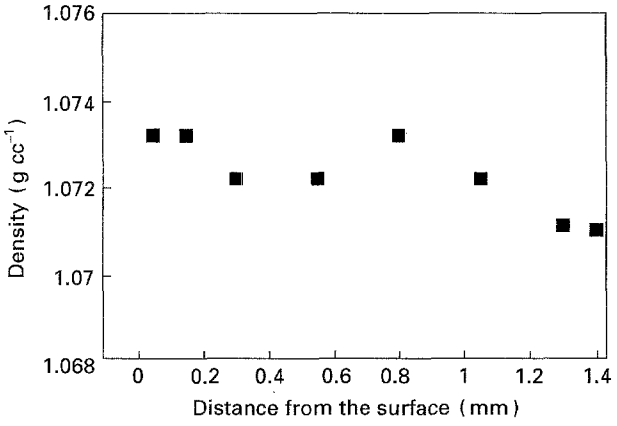


*Figure 4* Through the thickness density for as-moulded ABS dumbbell specimens.

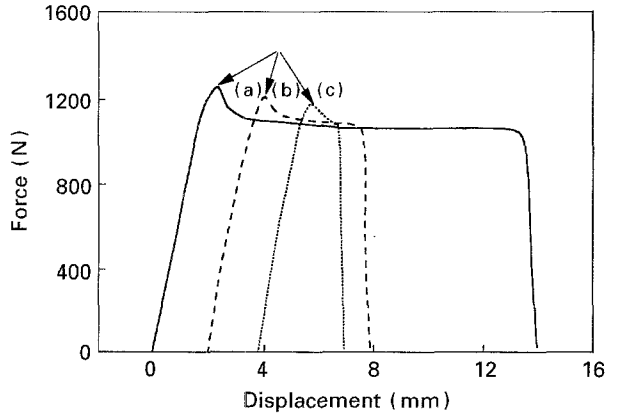


*Figure 5* Tensile force–displacement curves for the calculation of tensile yield strengths for: (a) as-moulded, (b) medium heat treated, and (c) full heat treated ABS specimens.

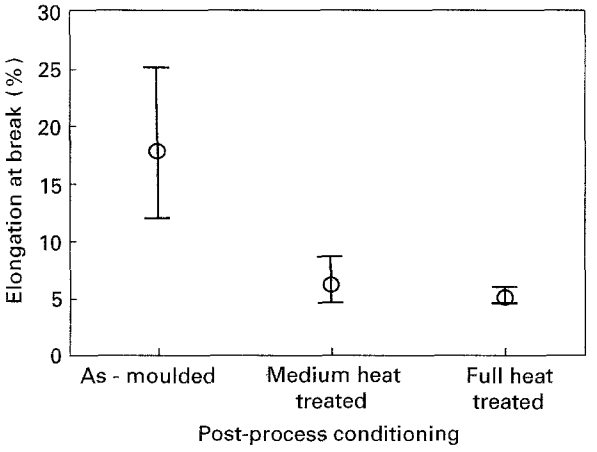


*Figure 6* Elongation at break versus post-process conditioning.

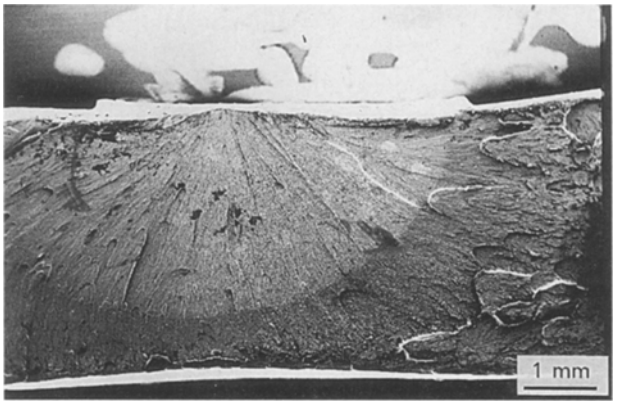


*Figure 7* SEM micrograph of tensile fracture surface of as-moulded ABS.

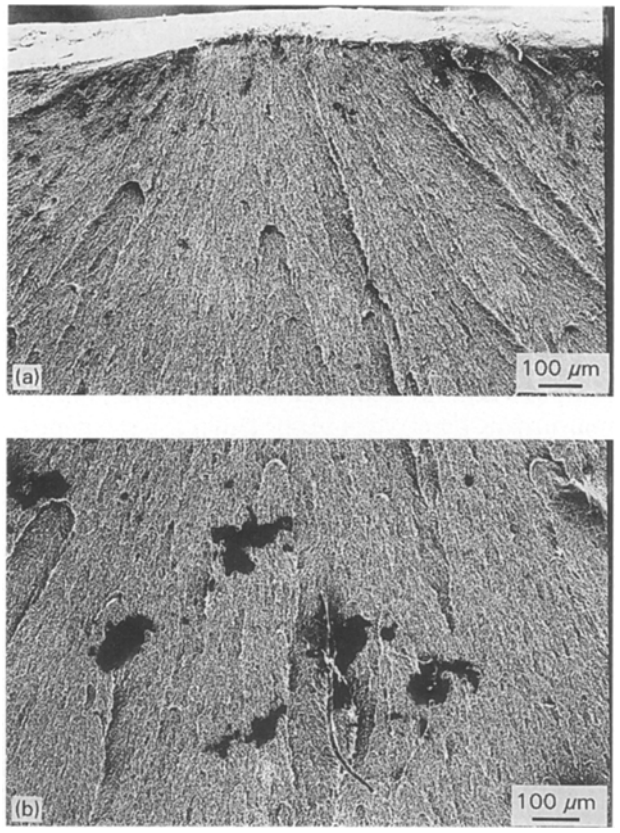


*Figure 8* SEM micrograph of tensile fracture surface of as-moulded ABS: (a) crack initiation, and (b) crack propagation.

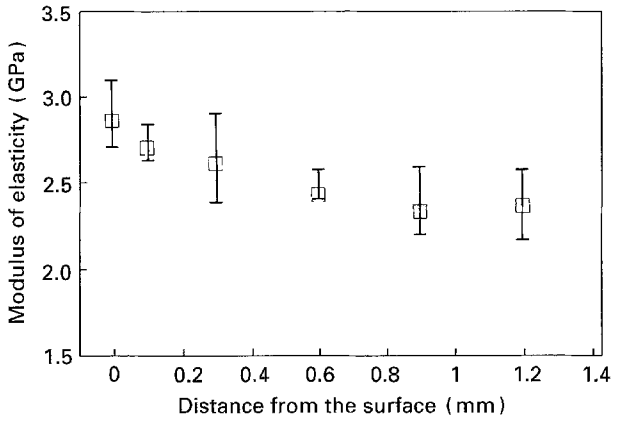


*Figure 9* Through the thickness modulus of elasticity for as-moulded ABS mouldings.

skin of the moulding. The compressive residual stresses obviously enhance the stiffness of the material under tensile load.

The flexural modulus and yield strength show slight improvement with heat treatment (see Figs 10 and 11; cf. Fig. 2).

## 3.2. Impact properties

The impact strength of ABS (see Fig. 12) is not significantly affected by the presence of residual stresses and molecular orientation. As-moulded and heat treated samples revealed similar force–deflection curves (see Fig. 13).

The impact fracture surface of ABS specimens is given in Figs 14–19. The figures consistently show the

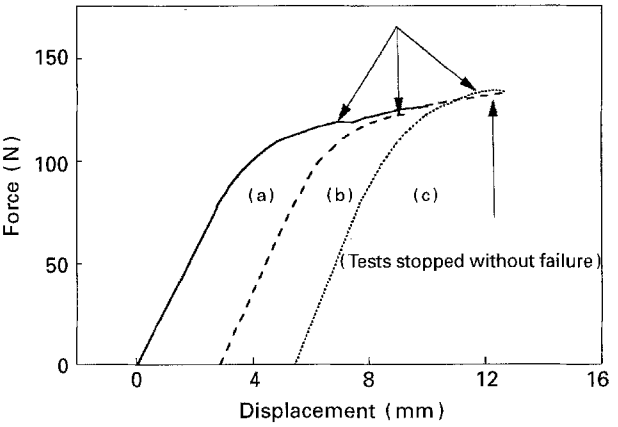


*Figure 10* Flexural load–deflection curves for the calculation of flexural yield strengths for: (a) as-moulded, (b) medium heat treated, and (c) full heat treated ABS specimens.

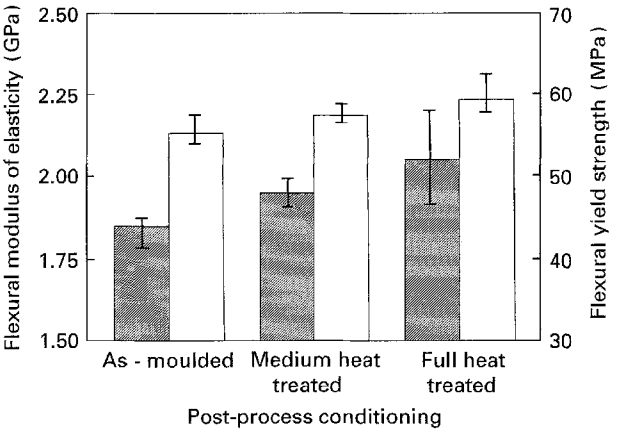


*Figure 11* Flexural properties versus post-process conditioning: (▩) flexural modulus of elasticity, and (□) flexural yield strength.

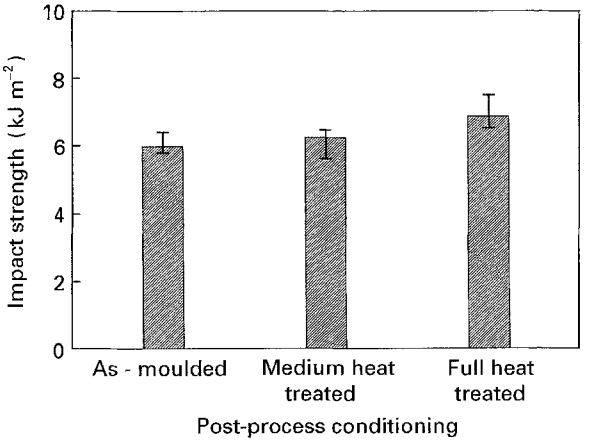


*Figure 12* Charpy impact strength versus post-process conditioning.

occurrence of smooth surfaces (indicating brittle failure) without the notch lines yielding or deforming for both as-moulded and heat treated samples. In the literature, similar brittle fracture surfaces are reported for polysulfone [8]. The impact strength of ABS is believed [13] to be affected by the loss peak of butadiene component of ABS, which occurs at $-90\,^{\circ}C$. The heat treatment significantly affected the transition behaviour of the butadiene component: heat

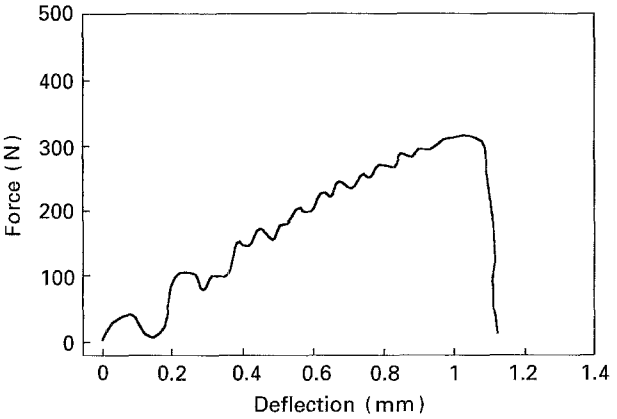


*Figure 13* Force–deflection diagram for the Charpy impact test of as-moulded ABS.

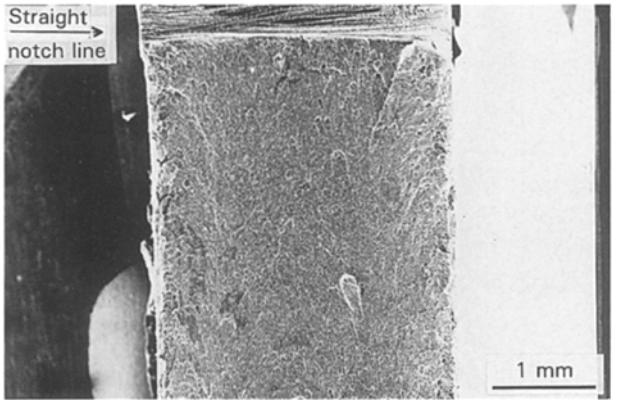


*Figure 14* SEM micrograph of Charpy impact fracture surface of as-moulded ABS.

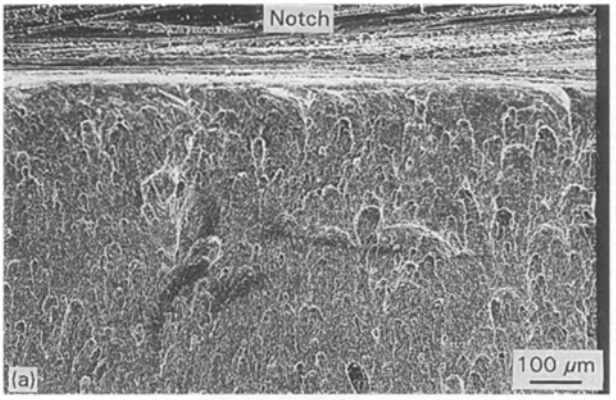


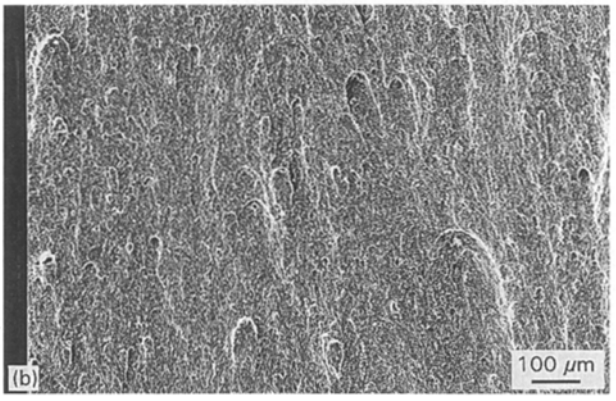


*Figure 15* SEM micrograph of Charpy impact fracture surface of as-moulded ABS: (a) crack initiation, and (b) crack propagation.

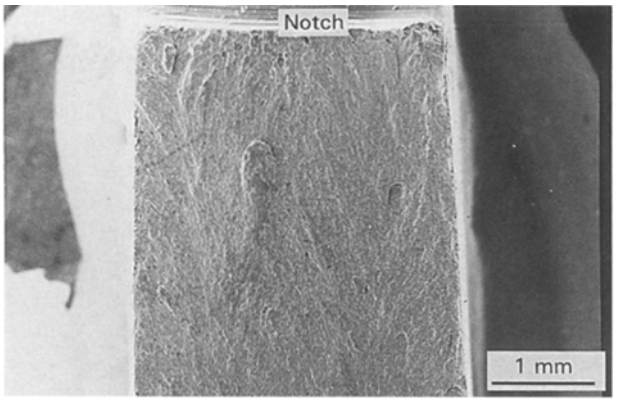


*Figure 16* SEM micrograph of Charpy impact fracture surface of medium heat treated ABS.

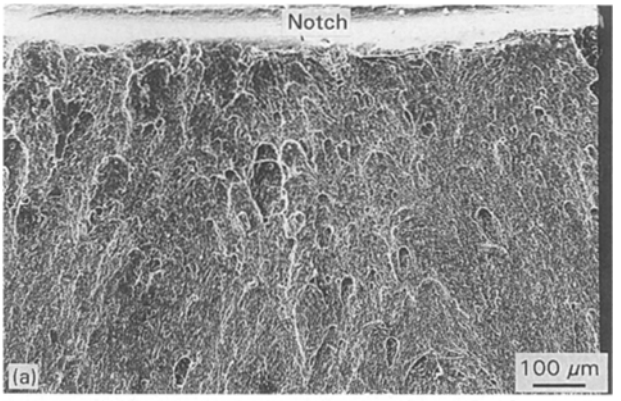


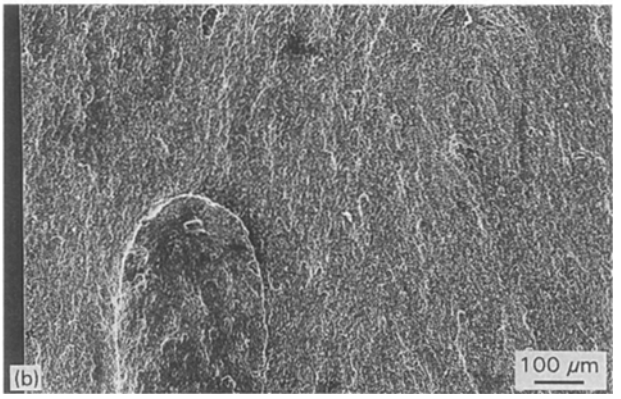


*Figure 17* SEM micrograph of Charpy impact fracture surface of medium heat treated ABS: (a) crack initiation, and (b) crack propagation.

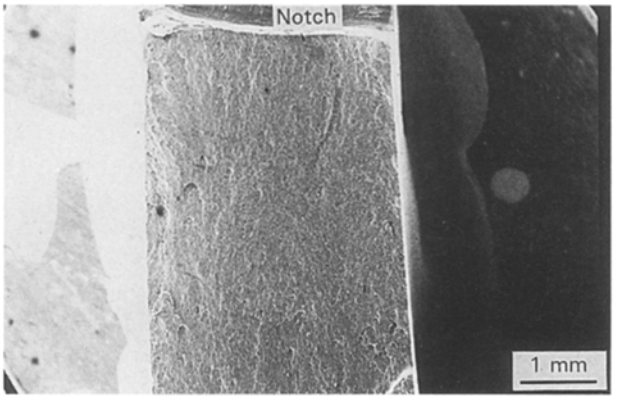


*Figure 18* SEM micrograph of Charpy impact fracture surface of full heat treated ABS.

treatment caused 9 °C reduction in the temperature of tan δ peak maximum and 13% increase in tan δ peak height (see Fig. 20). This may indicate that butadiene has a greater capacity to dissipate energy in annealed ABS specimens and, therefore, generates a slight improvement in Charpy impact strength.

The drop weight impact test results for as-moulded and heat treated ABS are given in Fig. 21 and a typical force–deflection trace is shown in Fig. 22. In contrast to the Charpy impact, the drop weight impact strength falls with heat treatment. The drop weight fracture surfaces of as-moulded and heat treated samples are presented in Figs 23–25. Large puncture openings

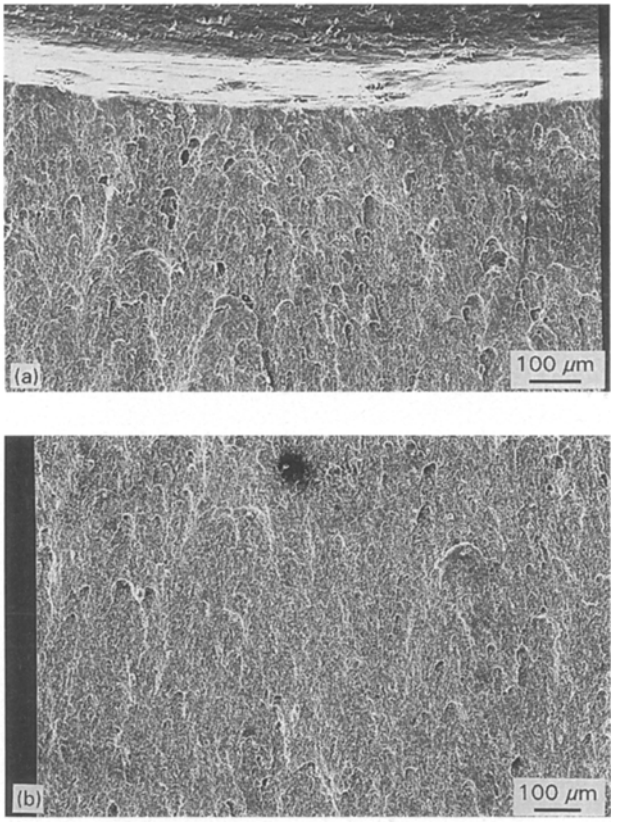


*Figure 19* SEM micrograph of Charpy impact fracture surface of full heat treated ABS: (a) crack initiation, and (b) crack propagation.

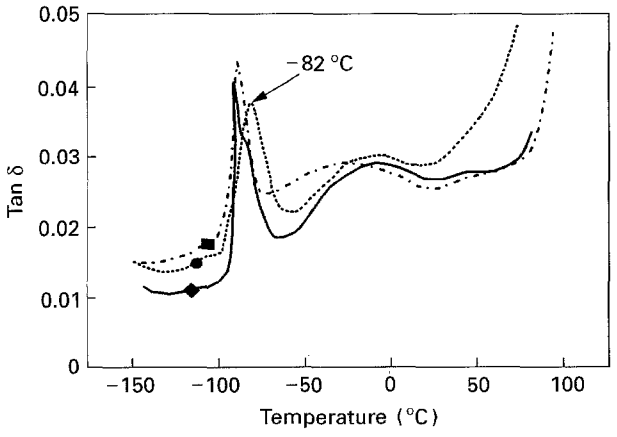


*Figure 20* The secondary loss peak (β transition) versus post-process conditioning for ABS: (●) as-moulded, (■) medium heat treated, and (◆) full heat treated specimens.

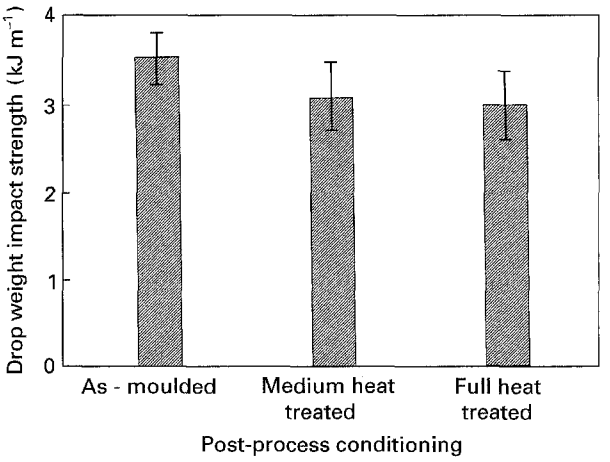


*Figure 21* Drop weight impact strength of ABS versus the post-process conditioning.

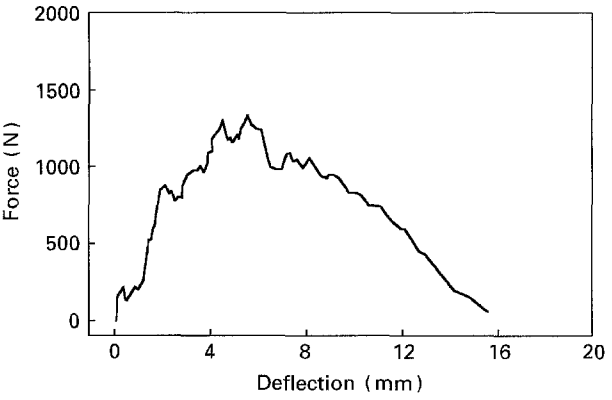


*Figure 22* Force–deflection trace for the drop weight impact test of as-moulded ABS.

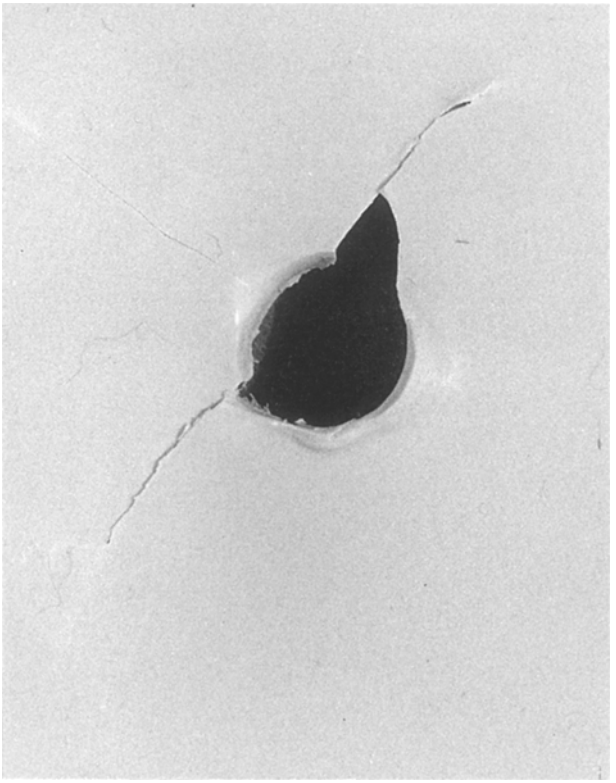

*Figure 23* The drop weight impact fracture surface (reverse side) of as-moulded ABS (2 × magnification).

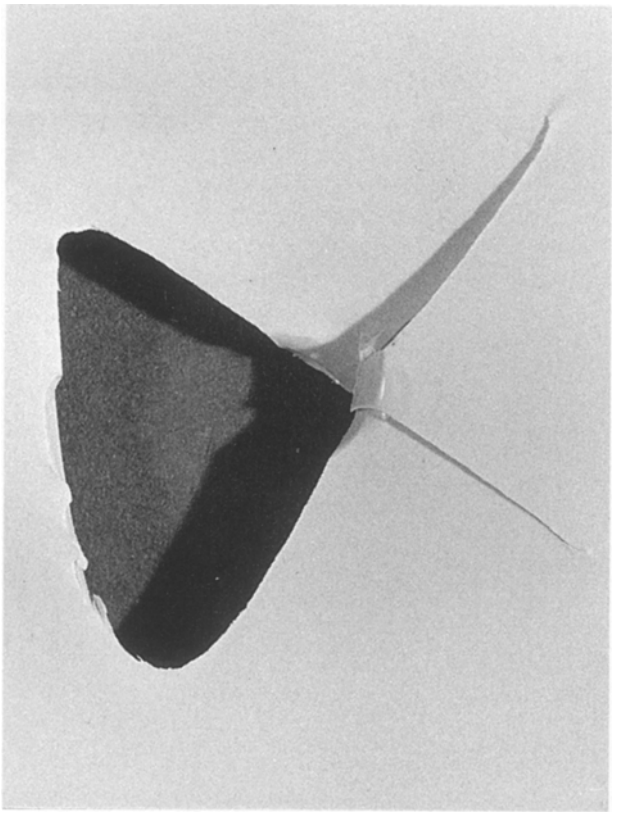

*Figure 24* The drop weight impact fracture surface (reverse side) of medium heat treated ABS (2 × magnification).

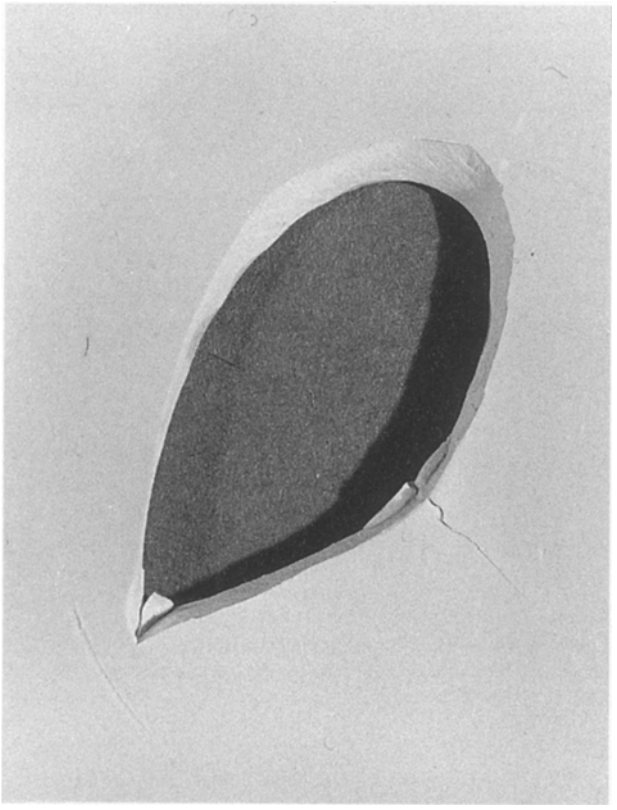

*Figure 25* The drop weight impact fracture surface (reverse side) of full heat treated ABS (2 × magnification).

were affected in both medium and full heat treated plaques, since the impacter caused brittle shattering. Conversely, the fracture openings in as-moulded plaques were almost confined to the size of the circumference of the plunger and indicated shear lips as a result of material yielding. In fact the plunger often got stuck in the as-moulded plaques. The drop weight impact behaviour is dictated by the ductility (see Fig. 5) of the material (there are no artificial cracks as in Charpy specimens to alter stress fields).

Although a decrease in the impact strength of extruded impact-modified polystyrene is reported [16] as the molecular orientation is reduced by increasing the processing temperature, the present results are indicative of the effect of the compressive residual stresses. As the residual stresses are relieved by medium heat treatment, the impact strength as well as the ductility of the samples is reduced. By contrast, further heat treatment did not cause any additional change in the properties. Probably the presence of compressive stresses at the surface retarded the development of the cracks and the material was allowed to yield before fracture.

## 3.3. Thermomechanical properties

Fig. 26 shows a typical dynamic mechanical thermal analysis (DMTA) curve of as-moulded ABS. Similar profiles, although with different magnitudes, were obtained for heat treated samples. The $T_g$ (defined as the temperature, where a maximum value in tan δ is indicated) and the maximum tan δ values (both as averages of five tests) for as-moulded and annealed ABS specimens are shown in Fig. 27. Annealing did not significantly affect the glass transition temperature. An approximately 2 °C increase in $T_g$ was observed with full heat treatment. A decrease was observed in the magnitude of the tan δ peak height at glass transition with full annealing, in agreement with the findings of Daane and Matsuoka [13] and Rohn and Herh [23] who showed that amorphous polymers with orientation and residual stresses resulted in higher tan δ values around $T_g$. Butadiene, the rubber component of ABS, generates a transition at − 90 °C, while the main glass transition of ABS (80–90 °C) is related to the stytrene–acrylonitrile component [13]. The maximum peak loss of as-moulded ABS is due to relaxation of back bone conformations of the orientated stytrene–acrylonitrile component [13]. As shown in Fig. 27, the magnitude of tan δ decreases at full heat

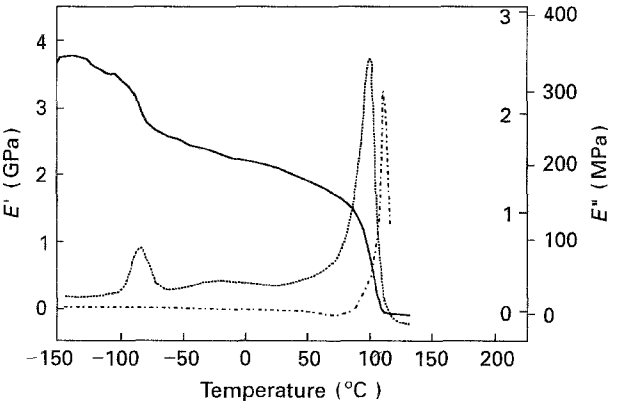


*Figure 26* The DMTA curves of as-moulded ABS: (—) $E'$, (.....) $E''$, and (–.–.–) tan $\delta$.

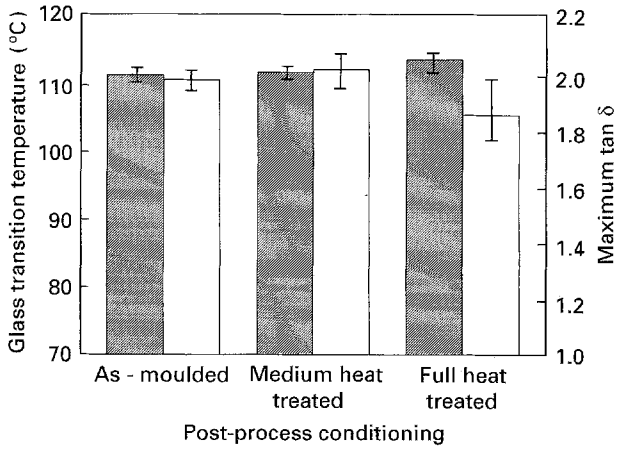


*Figure 27* Dynamic mechanical thermal properties versus post-process conditioning: (▩) $T_g$ and (□) maximum tan $\delta$ peak height.

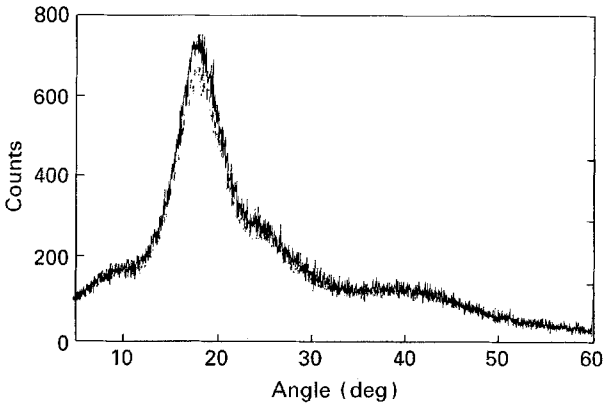


*Figure 28* Wide angle X-ray scattering patterns of as-moulded and annealed ABS specimens.

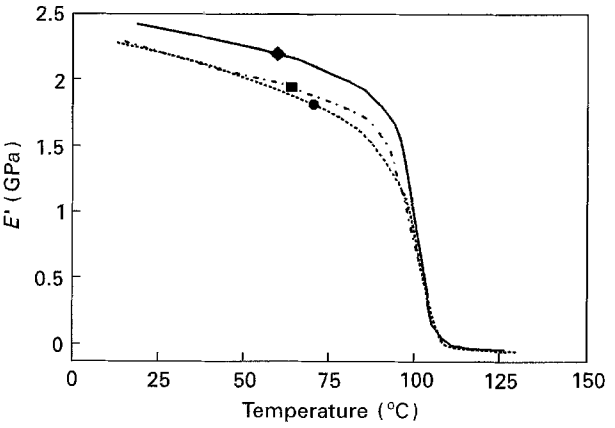


*Figure 29* Dynamic real modulus of elasticity versus post-process conditioning for: (●) as-moulded, (■) medium heat treated, and (◆) full heat treated specimens.

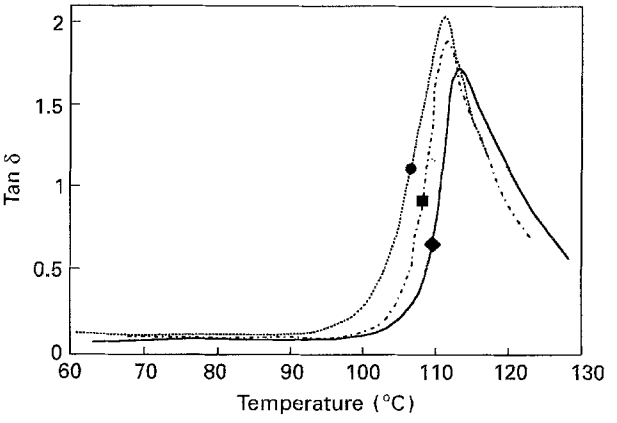


*Figure 30* Tan $\delta$ versus post-process conditioning for various ABS specimens at the glass transition region: (●) as-moulded, (■) medium heat treated, and (◆) full heat treated.

treatment, where the molecular orientation is recovered. The release of residual stresses by medium heat treatment did not change the peak loss significantly.

The second loss peak (due to butadiene) obtained at subambient conditions is shown in Fig. 20. A decrease of 7.5 and 9 °C at the position of this peak was observed for medium and full heat treated samples, respectively. Although the literature [13] indicates a third loss peak at − 130 °C for orientated specimens (the orientation was introduced in the as-moulded samples by cold drawing), the present work did not reveal any further peaks below − 90 °C. Wide angle X-ray scattering (WAXS) experiments were conducted in order to identify the occurrence of any structural variations as a result of post-processing conditioning. The associated WAXS patterns are presented in Fig. 28, and show no obvious variation between the various specimens.

The dynamic real modulus of elasticity results (Fig. 29) show that in the glass transition region (for example at 80 °C) the real modulus, $E'$, values for annealed specimens are significantly greater than those of as-moulded specimens: $E'$ values at approximately 80 °C are 1.8 GPa for as-moulded, 1.85 GPa for medium heat treated and 2.1 GPa for full heat treated specimens. As the specimens are slowly heated, during DMTA tests, through their glass transition temperature the residual stresses start to relax. The relaxation of the residual stresses in as-moulded specimens can stimulate the molecular relaxation associated with the glass transition and cause greater magnitudes of mechanical damping in the glass transition region as shown in Fig. 30. In full heat treated specimens there are no residual stresses or significant molecular orientation to relax and cause an early molecular movement and, thus, the stiffness of the material remains higher. The maintenance of higher $E'$ values near $T_g$, in annealed specimens, results in improved HDT performance as shown later.

The differences in the dynamic mechanical thermal properties of the specimens representing the skin and the core regions of ABS are presented in Fig. 31. The tests were carried out to determine through the thickness stiffness variation. Samples of 0.30 mm thicknesses were cut parallel to the mould fill direction from the dumbbell test mouldings.

The DMTA results between core and surface regions show a difference in tan $\delta$ peak values at glass transition. Although the temperature at which these peaks occur does not change through the moulding thickness (approximately 107 °C for both the surface and the core) the tan $\delta$ peak height was 1.56 for the core and 1.7 for the surface regions. The higher loss peak obtained at the surface may indicate the presence of greater molecular orientation in this region [26]. As

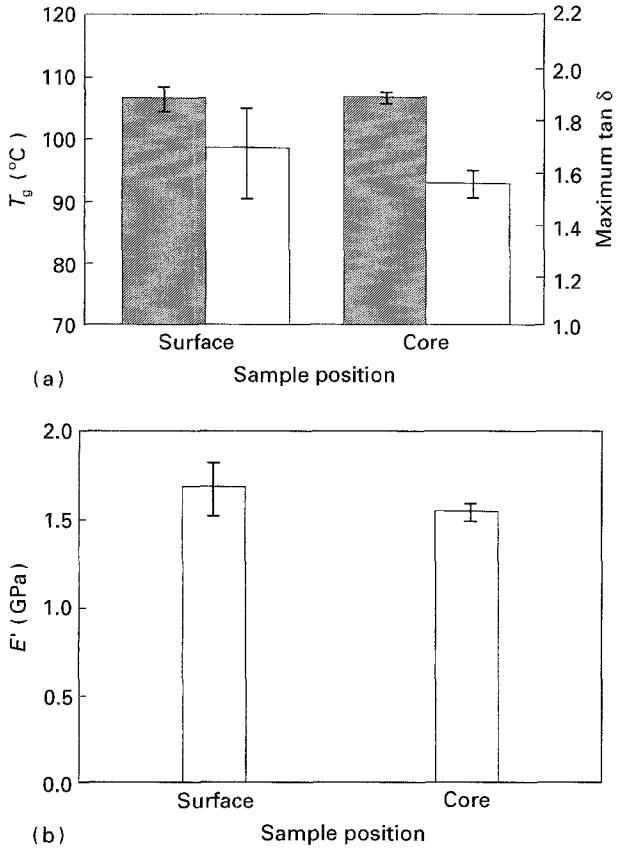


*Figure 31* Through the thickness dynamic mechanical thermal properties: (a) (▨) $T_g$, and (□) tan δ (b) E′.

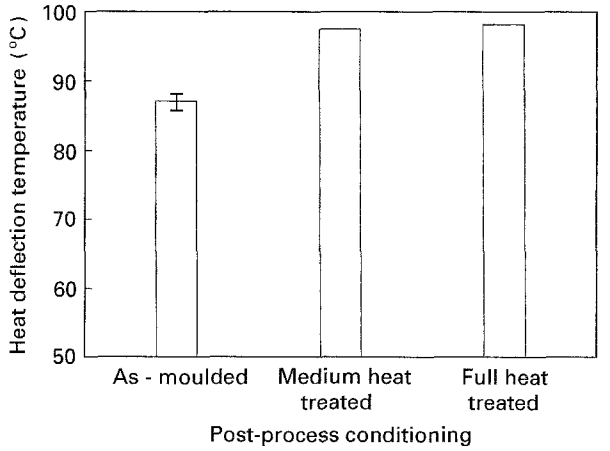


*Figure 32* Heat deflection temperature versus the post-process conditioning.

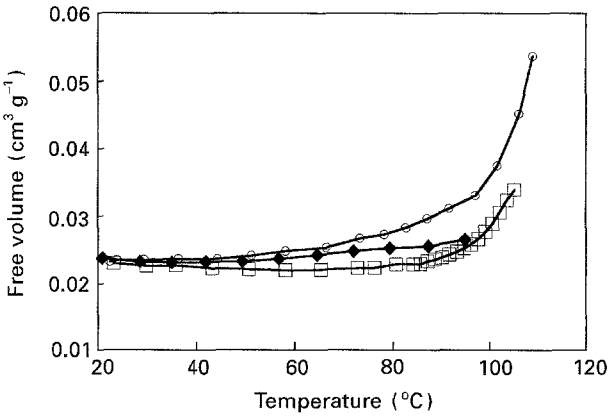


*Figure 33* Free volume versus temperature curves for: (□) as-moulded, (◆) medium heat treated, and (○) full heat treated ABS specimens.

would be expected the real modulus of elasticity at the surface is also higher than it is at the core.

Medium heat treatment results in an increase of 10 °C in HDT, and a further slight increase also results with full heat treatment as shown in Fig. 32. Thus, the presence of residual stresses rather than molecular orientation is the main factor affecting HDT. Siegmann *et al.* [2], without calculating the change in free volume, speculate that the increase in HDT is related to the decrease in free volume as a result of relaxation of residual stresses and molecular orientation. The results of the volume–temperature experiments indicate that annealing generates an increase in free volume in ABS mouldings (see Fig. 33). Therefore, there must be an alternative explanation for the higher stiffness values of annealed specimens around $T_g$. Both HDT and $E'$ results show an increase of stiffness around $T_g$ with heat treatment, and this improvement is thought to arise from the absence of residual stresses. The residual stresses and/or molecular orientation which are present in as-moulded specimens relax and, in turn, stimulate the molecular motion at the glass transition region during HDT and DMTA runs, resulting in earlier loss of stiffness (see Fig. 29 for relevant DMTA data).

The thermal variation of specific volume of as-moulded and heat-treated ABS specimens were determined using a length dilatometer, i.e. a thermal mechanical analyser (TMA), and then converting the coefficient of linear thermal expansion to the volumetric coefficient of expansion. The coefficient of volumetric thermal expansion, $\alpha_V$, can be determined from the coefficient linear thermal expansion, $\alpha$, for a temperature gradient, $\Delta T$, by the following equation

$$\alpha_V = [(1 + \Delta T\alpha)^3 - 1]/\Delta T \quad (1)$$

The specific volume as a function of temperature is calculated as follows

$$V = V_0(1 + \alpha_V \Delta T) \quad (2)$$

Where $V_0$, is the initial volume (at room temperature) and is calculated, using the inverse of the density of the specimen at room temperature.

It is notable that the change in specific volume in Fig. 34 is not completely linear. The specific volume results were compared with the predicted data. The theory assumes that the free volume is constant below $T_g$, and is a function of temperature above $T_g$. It is predicted [27] that the fraction of free volume below $T_g$ is about 1/40 of the total volume for most polymers. The predicted volume change in Fig. 34 was calculated using a constant coefficient of volumetric expansion at room temperature (obtained from experimental data as 0.0004 °C$^{-1}$) and 1/40 of the volume was subtracted from the total volume. In contrast to the free volume theory, the change in specific volume with temperature starts to deviate from a linear relationship as the temperature increases. The transition from glassy to rubbery region takes place

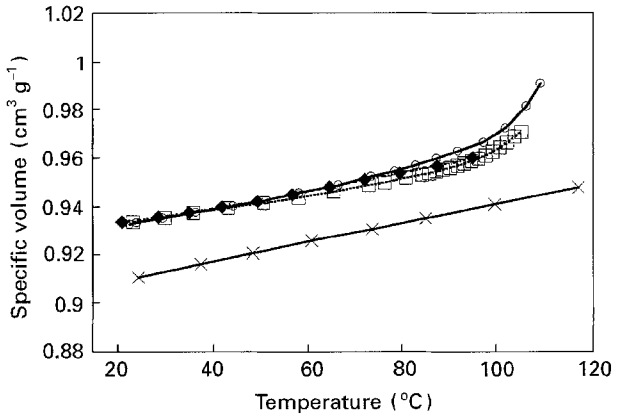


*Figure 34* Specific volume (measured by length dilatometer) versus temperature for: (□) as-moulded, (◆) medium heat treated and (○) full heat treated ABS specimens, and (X) calculated results using a constant coefficient of volumetric thermal expansion.

over a wide temperature range. The free volume is considered to be equal to the difference between the magnitude of the measured and calculated curves in Fig. 34.

The free volume estimations for as-moulded and heat treated ABS samples is given in Fig. 33. Although the resultant amount of the total free volume may not be completely correct for the assumption that 1/40 of the total volume is equal to free volume below $T_g$, the free volume versus the temperature diagram clearly demonstrates the non-linear expansion of the free volume.

It is proposed that compressive residual stresses at the surface tend to decrease the free volume, while tensile residual stresses at the interior tend to increase it by pulling apart the molecules [2]. However, it is also reported that the free volume decreases as the molecules are oriented [27]. Similarly the TMA results show (Figs 33 and 34) that the free volume increases after the relaxation of residual stresses and molecular orientation.

## 4. Conclusions

The effects of residual stresses and molecular orientation on the properties of injection moulded acrylonitrile–butadiene–styrene (ABS) is examined by conducting tests on as-moulded and annealed specimens. Annealing below the glass transition temperature, $T_g$, at approximately 80 °C (medium heat treatment), removes much of the residual stresses. The tensile modulus of elasticity, flexural modulus of elasticity and flexural yield strength of medium heat treated ABS increase by 4, 5 and 4%, respectively. The magnitude of variations in these mechanical properties increases to approximately 11, 10 and 7% respectively, as a result of a further heat treatment above $T_g$, at 135 °C (full heat treatment). An increase of 0.11% in material density is affected by full heat treatment.

The heat treatment changes the tensile failure mode of the mouldings by influencing the state of the residual stresses. The ductility (as indicated by elongation to failure) decreases by about 180% upon medium heat treatment. Further annealing causes an additional drop of 20%.

The changes in the impact strength of as-moulded and annealed ABS is not significant where the Charpy impact strength is increased from 6 to 7 kJ $m^{-2}$ following heat treatment, while the drop weight strength is decreased from 3.5 to 3.0 kJ $m^{-1}$.

The medium heat treated specimens indicate improvements of approximately 10 °C in heat distortion temperature (HDT). This coincides with an approximately 17% increase in dynamic real modulus, $E'$, of the annealed specimens in the vicinity of HDT.

Annealing does not significantly affect the glass transition temperature (defined as the temperature of the maximum tan δ). However, a progressive decrease was observed in the magnitude of the tan δ peak height at glass transition with annealing.

## References


1. P. C. POWELL, "Engineering with Polymers" (Arrowsmith Ltd, Bristol, 1983) pp. 254–8.
2. A. SIEGMANN, M. NARKIS and N. ROZENWEIG, *Polym. Eng. Sci.* **19** (1979) 223.
3. P. SO and L. J. BROUTMAN, *ibid.* **16** (1976) 785.
4. L. E. HORNBERGER and K. L. DEVRIES, *ibid.* **27** (1987) 1473.
5. Y. YAMAGUCHI, Y. OYANAGI and Y. OZAKI, *Kobunshi Ronbushu, Eng. Ed.* **4** (1975) 507.
6. L. J. BROUTMAN and S. M. KRISHNAKUMAR, *Polym. Eng. Sci.* **16** (1976) 74.
7. G. A. CAMPBELL, S. SETTLEMIRE, K. KLEWICKI, T. KENNY, J. D. SMALL and J. D. FRICKE, *SPE ANTEC Tech. Papers* **35** (1989) 312.
8. J. F. MANDELL, K. L. SMITH and D. D. HUANG, *Polym. Eng. Sci.* **21** (1981) 1173.
9. L. HOARE and D. HULL, *ibid.* **17** (1977) 204.
10. V. F. DALAL and A. MOET, *ibid.* **28** (1988) 544.
11. T. T. JONES, *Pure Appl. Chem.* **45** (1976) 41.
12. D. G. LEGRAND, *J. Appl. Polym. Sci.* **13** (1969) 2129.
13. J. H. DAANE and S. MATSUOKA, *Polym. Eng. Sci.* **8** (1968) 246.
14. P. I. VINCENT, *Polymer* **15** (1974) 111.
15. P. H. C. SHU, *SPE ANTEC Tech. Papers* **35** (1989) 393.
16. P. HEIDEMEYER, G. MENGES and W. MICHAELI, *ibid.* (1989) 688.
17. R. BOUKHILI, R. GAUVIN and M. GOSSELIN, *ibid.* (1989) 1566.
18. E. S. CLARK, *Appl. Polym. Sympos.* **24** (1974) 45.
19. V. TAN and M. R. KAMAL, *J. Appl. Polym. Sci.* **22** (1978) 2341.
20. Z. CHEN and J. R. WHITE, *Plast. Rubber Compos. Process. Appl.* **18** (1992) 289.
21. M. R. KAMAL and P. G. LAFLEUR, *Polym. Eng. Sci.* **26** (1986) 103.
22. E. FLEISCHMANN, *Int. Polym. Process* **4** (1989) 158.
23. C. ROHN and P. HERH, *SPE ANTEC Tech. Papers* **34** (1988) 1135.
24. S. OZDEN, PhD thesis, University of Ulster at Jordanstown (1994).
25. J. G. CRACKNELL, PhD thesis, University of Ulster (1993).
26. B. O'DONNEL, PhD thesis, University of Newcastle Upon Tyne (1989).
27. F. W. BILLMEYER, "Textbook of Polymer Science", 2nd Edn, (Wiley, London, 1971) p. 210.



*Received 28 June*
*and accepted 16 November 1994*